Available online at www.sciencedirect.com
SCIENCE DIRECT
Journal of Chromatography A, 1099 (2005) 136–148
JOURNAL OF CHROMATOGRAPHY A
www.elsevier.com/locate/chroma

Extrathermodynamic interpretation of retention equilibria in reversed-phase liquid chromatography using octadecylsilyl-silica gels bonded to C_1 and C_{18} ligands of different densities

Kanji Miyabe [a], Georges Guiochon [b,c,*]

[a] *Faculty of Engineering, Toyama University, 3190, Gofuku, Toyama 930-8555, Japan*
[b] *Department of Chemistry, The University of Tennessee, Knoxville, TN 37996-1600, USA*
[c] *Division of Chemical Sciences, Oak Ridge National Laboratory, Oak Ridge, TN 37831, USA*

Received 15 June 2005; received in revised form 26 August 2005; accepted 1 September 2005
Available online 29 September 2005

Abstract

The retention behavior on silica gels bonded to C_{18} and C_1 alkyl ligands of different densities was studied in reversed-phase liquid chromatography (RPLC) from the viewpoints of two extrathermodynamic relationships, enthalpy–entropy compensation (EEC) and linear free energy relationship (LFER). First, the four tests proposed by Krug et al. were applied to the values of the retention equilibrium constants (K) normalized by the alkyl ligand density. These tests showed that a real EEC of the retention equilibrium originates from substantial physico-chemical effects. Second, we derived a new model based on the EEC to explain the LFER between the retention equilibria under different RPLC conditions. The new model indicates how the slope and intercept of the LFER are correlated to the compensation temperatures derived from the EEC analyses and to several parameters characterizing the molecular contributions to the changes in enthalpy and entropy. Finally, we calculated K under various RPLC conditions from only one original experimental K datum by assuming that the contributions of the C_{18} and C_1 ligands to K are additive and that their contributions are proportional to the density of each ligand. The estimated K values are in agreement with the corresponding experimental data, demonstrating that our model is useful to explain the variations of K due to changes in the RPLC conditions.

Keywords: Ligand density in RPLC; Extrathermodynamic relationship; Retention mechanism; Reversed phase liquid chromatography

1. Introduction

Octadecylsilyl (C_{18})-bonded silica gels are the most popular type of packing materials for RPLC [1,2]. Their chromatographic behavior depends on the modification conditions of the C_{18} and C_1 ligands bonded to the base silica gels, for instance on the density and type (monomeric or polymeric) of C_{18} ligands, and on the end-capping treatment with C_1 ligands for residual silanol groups. In some cases, the modification conditions of C_{18} and C_1 ligands are made intentionally in order to attain specific separations.

The influence of the alkyl ligand density on the chromatographic behavior has been studied from the viewpoint of the retention equilibrium [3–8]. In some papers [4–6], linear correlations have been observed between the retention factor (k') and the alkyl ligand density at low density conditions. It was reported that, although κ' initially increases with increasing density of the alkyl ligands, it tends toward a constant level at high ligand densities [4–6]. Limit values of κ' were observed for small sample compounds at high ligand densities [4]. However, the correlations between κ' and the alkyl ligand density become more nearly linear with increasing molecular size of the sample compounds or with decreasing length of the alkyl chain [4,5]. The value of κ' does not begin to plateau when the sample molecules are large enough [4]. The influence of the alkyl ligand density on the separation factor (α_{sep}) was also studied [7,8]. It was reported that the values of α_{sep} for a methylene or a phenyl unit are linearly correlated with the surface coverage of C_{18} ligands, although the increment in α_{sep} for one methylene group is relatively small [8].

The retention equilibrium in RPLC has also been studied from the thermodynamic and the extrathermodynamic points of view. The temperature dependence of κ' was analyzed using the van't

* Corresponding author. Tel.: +1 8659740733; fax: +1 8659742667.
E-mail address: guiochon@ion.chem.utk.edu (G. Guiochon).

0021-9673/$ – see front matter © 2005 Elsevier B.V. All rights reserved.
doi:10.1016/j.chroma.2005.09.001

Hoff equation to derive the changes in the enthalpy (ΔH) and entropy (ΔS) associated with the adsorption of sample molecules from the mobile phase onto the stationary phase. Analyses of retention equilibrium data are supported by a solid theoretical basis, i.e., the thermodynamics of phase equilibria. Extrathermodynamic correlations between thermodynamic parameters have also been studied to discuss retention and separation mechanisms in RPLC. For instance, mechanistic similarities of the retention behavior in RPLC were discussed on the basis of the enthalpy–entropy compensation (EEC) between ΔH and ΔS. Numerous publications have demonstrated an EEC on experimental data [9–20] and supported the possibility of an EEC on theoretical bases [21–25]. Compensation temperatures (T_c) between ca. 500 and 1000 K have been reported for retention equilibria under different RPLC conditions, different mobile phase solvents, sample compounds, and temperature ranges [10,11,15,17–20]. The existence of an EEC suggests that the retention behavior is governed by a single mechanism.

We have also studied the influence of the C_{18} ligand density on some RPLC characteristics [18,26]. With increasing density of C_{18} ligand, the retention equilibrium constant (K), the absolute value of the isosteric heat of adsorption (the enthalpy change due to retention) (Q_{st}), and the activation energy of surface diffusion increase while, in contrast, the surface diffusion coefficient decreases. There is a critical carbon content of the stationary phase above which these four parameters no longer significantly change with increasing C_{18} ligand density. This level probably depends on the size of the sample molecules. It was also suggested that one sample molecule probably interacts with a single C_{18} chain at low C_{18} ligand densities whereas all the C_{18} ligands do not necessarily contribute to the retention behavior of the sample molecules at high ligand densities. The possibility of the interaction of one sample molecule with several C_{18} ligands was denied even when the density of C_{18} ligand is high enough [26]. An explanation for the retention behavior on C_{18}-silica gels is the assumption that the sample molecules penetrate into the layer of C_{18} ligands [27,28]. However, the actual retention behavior in RPLC could be more complicated and we have not yet sufficiently interpreted the influence of the modification conditions of the stationary phase, i.e., the length and density of alkyl ligands, on retention equilibria, notably from the thermodynamic and extrathermodynamic viewpoints.

This paper is concerned with the retention behavior of several C_{18}-bonded silica gels the surface of which is modified with C_{18} and C_1 ligands at different densities. First, it was attempted to explain the experimental retention data of sample molecules on the C_{18} ligands on the basis of the solvophobic theory. We assumed independently parallel contributions of the C_{18} and C_1 ligands on the retention equilibrium. Then, we introduced a new coefficient, κ, the equilibrium constant K normalized by the alkyl ligand density (σ), because the densities of both the C_{18} and the C_1 ligands is changed in this study. We tried to demonstrate the presence of a true EEC relationship for the retention equilibrium in RPLC by analyzing the temperature dependence of κ, according to the four methods proposed by Krug et al. [21–23]. Finally, we derived a new model to account for the influence of several experimental parameters on the retention behavior in RPLC. It was demonstrated that the new model provides a comprehensive interpretation of the variations of K with some RPLC conditions.

2. Experimental

2.1. Columns

Table 1 lists some physico-chemical properties of the stationary phases, i.e., five C_{18}-silica gels (ODS, #1–#5) and one C_1-silica gel (TMS, #6). The RPLC columns packed with these separation media and most of the information were obtained from YMC (Kyoto, Japan). All the stationary phases are synthesized from the same base silica gel. The five C_{18}-silica gels are probably monomeric type packing materials. The density of C_{18} ligand was calculated from the carbon content of the packing materials and the BET surface area of the base silica gel (290 $m^2\,g^{-1}$). The carbon content of the C_{18}-silica gels from #1 to #4 increased from 0.9 to 3.4 wt.% upon end-capping treatment with trimethylsilyl ligands. The end-capping caused no substantial increase in the carbon content of the C_{18}-silica gel #5.

The density of C_{18} ligand was estimated in the range between 0.26 and 3.2 $\mu mol\,m^{-2}$. Although this range is not extremely

Table 1
Physico-chemical properties of RP stationary phases

Packing material/column no.	1	2	3	4	5	6
Main alkyl chain	C_{18}	C_{18}	C_{18}	C_{18}	C_{18}	C_1
Particle density, ρ_p ($g\,cm^{-3}$)	0.67	0.69	0.71	0.79	0.86	0.74
Porosity (ε_p)	0.65	0.61	0.57	0.50	0.46	0.62
Carbon content (%)						
Before end-capping	1.6	3.6	6.4	12.8	17.1	4.1
After end-capping	5.0	6.6	8.6	13.7	17.1	–
C_1 ligand, C_{C_1}	3.4	3.0	2.2	0.9	0	4.1
C_{18} ligand density, $\sigma_{C_{18}}$ ($\mu mol\,m^{-2}$)[a]	0.26	0.59	1.1	2.3	3.2	–
Distance between C_{18} ligands (nm)[a]	2.9	1.9	1.4	1.0	0.81	–
Ratio of silanol group treated with C_{18} ligands (%)[b]	3.2	7.3	13	29	40	–

[a] Calculated from the carbon content before end-capping and the BET surface area of the base silica gel (290 $m^2\,g^{-1}$).
[b] Calculated from the C_{18} ligand density and the density of silanol groups on the surface of the base silica gel (assumed to be 8 $\mu mol\,m^{-2}$).

high, it sufficiently covers the practical conditions concerning the density of C_{18} ligands on RPLC stationary phases because the highest density of C_{18} ligands is probably about 3.0–3.5 μmol m^{-2} for most commercially available monofunctional C_{18} packing materials. It is estimated that about 40% of the silanol groups react with the C_{18} ligands on the surface of the base silica gel [29] to form the C_{18}-silica gels #5 (density 3.2 μmol m^{-2}) since the typical density of silanol groups is about 8 μmol m^{-2}. The average distance between adjacent C_{18} ligands on the surface of the C_{18}-silica gels was calculated from the density of the C_{18} ligands. This distance is likely to be about one to four times the average molecular size of the sample molecules. For instance, the molecular radii of benzene and *n*-hexylbenzene are respectively estimated at about 0.34 and 0.45 nm from their molar volumes at their normal boiling point, assuming a spherical molecular shape.

2.2. Apparatus

A high performance liquid chromatograph system (LC-6A, Shimadzu, Kyoto, Japan) was used for acquiring experimental data. A Rheodyne (Cotati, CA, USA) valve injector (Model 7125) was used for injecting small amounts of the sample solution (ca. 0.5–300 μl) into the column. The column temperature was kept constant by immersing it in temperature-controlled water. The ultraviolet detector of the HPLC system was used for monitoring the concentration of the sample compounds in the effluent at the column exit.

2.3. Chromatographic measurements

The mobile phase was a methanol/water mixture (70/30, v/v). Alkylbenzenes (ethylbenzene, *n*-butylbenzene, and *n*-hexylbenzene) were used as the sample compounds. Uracil and sodium nitrate were used as inert tracers. They were all reagent grade and used without further purification. Sample solutions (ca. 0.1 wt.% in most cases) were prepared by dissolving the sample compounds into the mobile phase. The elution peak profiles were measured by means of the pulse response experiment (i.e., elution chromatography) at different mobile phase flow rates (1.0–2.0 m/min^{-1}). The column temperature was changed in the range from 288 to 308 K.

2.4. Data analysis

The value of K was calculated from the first moment (μ_1) of the elution peak, which is the same as the retention time when the peak profile is symmetrical. According to the moment theory, μ_1 is formulated as follows.

$$\mu_1 = \left(\frac{L}{u_0}\right)[\varepsilon_e + (1-\varepsilon_e)(\varepsilon_p + \rho_p K)] \quad (1)$$

where L is the column length, u_0 the superficial velocity of the mobile phase, ε_e and ε_p the external and internal porosities, respectively, and ρ_p is the particle density. Details regarding the moment analysis method can be found in the literature [18,30–33].

In order accurately to derive K from μ_1, the residence time of the sample compounds in the extra-column tubes was subtracted from the experimental values of μ_1 [18,33]. Similar pulse response experiments were made without the column to measure the internal volume of the extra-column pipes between the injection valve and the column and between the column and the detector. On the other hand, the contribution of μ_1 of the sample pulses introduced at the inlet of the column was neglected because of the extremely small size of the sample solution injected. As described above, for instance, the injection volume of the sample solution of *n*-hexylbenzene was ca. 300 μl because of the low solubility of the compound in the mobile phase, which is not small compared with conventional sample volumes in LC. However, the retention volume of *n*-hexylbenzene is at least two orders of magnitude larger than the injection volume. The retention of *n*-hexylbenzene is so strong that the volume of the sample injected provides substantially no influence on the first moment analysis of the elution peaks.

3. Results and discussion

Contribution of C_{18} and C_1 ligands to K. Fig. 1 shows the correlation of the experimental values of K (K^{exp}) at 298 K with the carbon content (C) of the RPLC stationary phases. The superscript^{exp} denotes chromatographic data measured in the RPLC systems. The value of K^{exp} increases with increasing C for all the sample compounds. However, the slope of the correlations between K^{exp} and C gradually decreases with increasing C. Almost the same values of K^{exp} are observed for the two C_{18}-silica gel columns #4 and #5. The trend of the curves in Fig. 1 is similar to that of the correlation between K and the alkyl chain length in RPLC [18]. The value of K for relatively small molecular size sample compounds begins to plateau in the range of the alkyl chain length longer than around C_8. It was concluded that only part of longer alkyl ligands might contribute to the

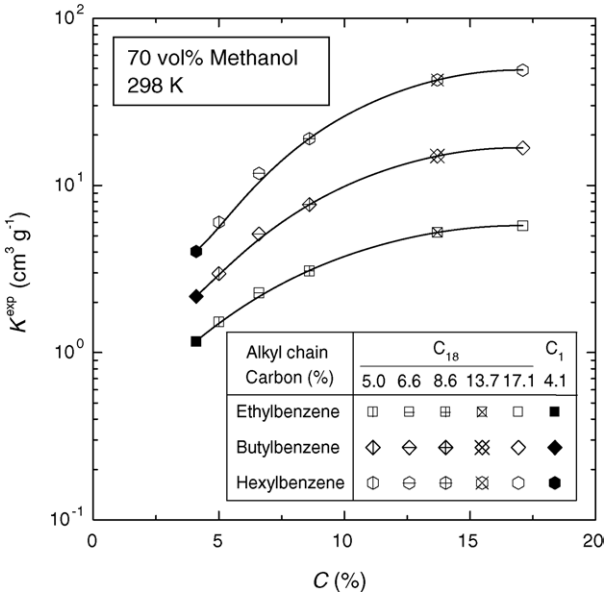

Fig. 1. Correlation of K^{exp} with C of the stationary phases.

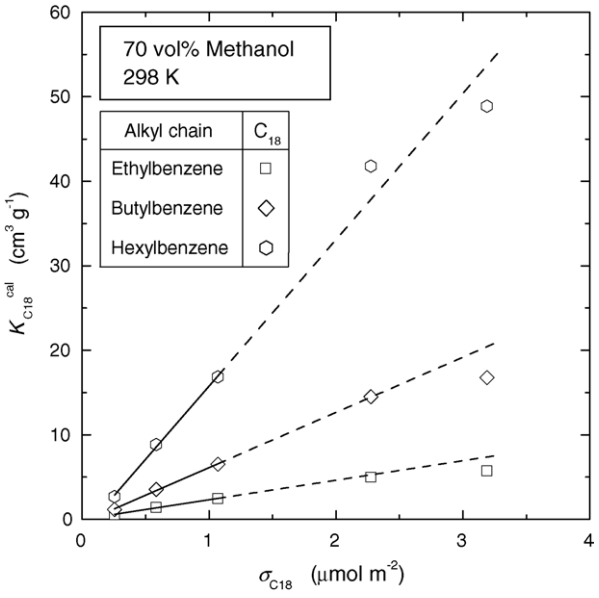

Fig. 2. Plot of $K_{C_{18}}^{cal}$ against $\sigma_{C_{18}}$.

retention behavior in RPLC [18]. Similarly, the results in Fig. 1 suggests that all the C_{18} ligands do not necessarily contribute to the retention of the sample compounds at high coverage density of C_{18} ligands [26].

In order to clarify the characteristics of the retention behavior on the C_{18}-silica gel columns (#1–#5) which are all packed with C_{18}-silica gels treated with trimethylsilyl ligand for end-capping, it was assumed as a first approximation that the value of K consists of the sum of the contributions of the C_{18} ligands ($K_{C_{18}}$) and of the C_1 ligands (K_{C_1}) and that the contribution of the C_1 ligands is proportional to the corresponding carbon content (C_{C_1}).

$$K = K_{C_1} + K_{C_{18}} \tag{2}$$

$$K_{C_1} = K_{TMS}^{exp}\left(\frac{C_{C_1}}{4.1}\right) \tag{3}$$

where K_{TMS}^{exp} denotes the retention equilibrium constant of the sample compounds measured on the C_1-silica gel column (#6). The subscripts C_1 and C_{18} stand for the respective contributions of the C_1 and C_{18} ligands to the retention. As listed in Table 1, the value of C for the C_1-silica gel (#6) is 4.1 wt.%.

The open symbols in Fig. 2 represent the contributions $K_{C_{18}}^{cal}$ as a function of the density of the C_{18} ligand ($\sigma_{C_{18}}$). The superscript (cal) stands for calculated values. The values of $K_{C_{18}}^{cal}$ are derived according to Eqs. (2) and (3) from K^{exp} measured using the four C_{18}-silica gel columns (#1–#4), K_{TMS}^{exp}, and C_{C_1}. There are two reasons to assume that K_{C_1} is linearly correlated with σ_{C_1} (hence, C_{C_1}) in the above calculation. First, the molecular size of the sample compounds is larger than that of the C_1 ligand but smaller than that of the C_{18} ligand. It is predicted that a linear correlation is observed between K_{C_1} and σ_{C_1}, and, in contrast, a more curved one between $K_{C_{18}}$ and $\sigma_{C_{18}}$. In an earlier paper [5], Unger et al. prepared many silica gel packing materials bonded with alkyl ligands of different chain lengths (C_1, C_4, C_6, C_8, and C_{18}) and ligand densities (0–4.1 μmol m^{-2}) with no end-capping treatment. They correlated κ' of dimethylaniline and benzoic acid butyl ester for each stationary phase with the alkyl ligand density. As expected, almost linear correlations were observed between K_{C_1} and σ_{C_1}. On the other hand, the curved profiles observed between $K_{C_{18}}$ and $\sigma_{C_{18}}$ became nearly linear correlations at low $\sigma_{C_{18}}$. Second, the contribution of the C_1 ligand (K_{C_1}) to K is smaller than that of the C_{18} ligand ($K_{C_{18}}$), except for the C_{18}-silica gel #1. It seems that the calculation error originating from the assumption of a linear correlation between K_{C_1} and σ_{C_1} is smaller than that between $K_{C_{18}}$ and $\sigma_{C_{18}}$.

As described above, Fig. 2 also shows linear correlations between $K_{C_{18}}^{cal}$ and $\sigma_{C_{18}}$ at low C_{18} ligand densities.

$$K_{C_{18}} = \alpha'\sigma_{C_{18}} + \beta' \tag{4}$$

where α' and β' are numerical coefficients. The solid lines are calculated from the plots for the three C_{18}-silica gels of low $\sigma_{C_{18}}$ (#1–#3) because it is expected that the $K_{C_{18}}^{cal}$ values for these three stationary phases account more accurately for the contribution of a single C_{18} ligand to $K_{C_{18}}$ under the conditions that one sample molecule interacts with one C_{18} alkyl ligand. The manner of the steric interactions between the sample molecules and the C_{18} chains depends on the density of the C_{18} ligands. When $\sigma_{C_{18}}$ is large enough, it is probable that the sample molecules penetrate into the layer of bonded C_{18} ligands [27,28]. However, it would be much harder for sample molecules to make contact with several C_{18} ligands on the C_{18}-silica gels of low $\sigma_{C_{18}}$.

In Fig. 2, the dashed lines are extrapolation of the corresponding solid lines. The values of $K_{C_{18}}^{cal}$ on the C_{18}-silica gel #4 seem to lay on the dashed lines while the $K_{C_{18}}^{cal}$ values for the C_{18}-silica gel #5 are lower than predicted by the dashed lines. The estimated average distance between two C_{18} ligands is comparable to the molecular size of the sample compounds on both C_{18}-silica gels #4 and #5, as listed in Table 1 whereas the distance calculated for the C_{18}-silica gel #1 is several times larger than the size of the sample molecules. Although the estimates of the average distance between two C_{18} ligands on the C_{18}-silica gels #4 and #5 are comparable to the molecular size of the sample compounds, the structural flexibility of the C_{18} chains may allow interactions of the sample molecules with several C_{18} ligands. If multiple interactions actually take place, the values of $K_{C_{18}}^{cal}$ for the C_{18}-silica gels #4 and #5 would be larger than predicted by the dashed lines in Fig. 2, a prediction inconsistent with the data in Fig. 2.

On the other hand, $K_{C_{18}}^{cal}$ increases almost linearly with increasing C_{18} chain density at low $\sigma_{C_{18}}$. The results in Fig. 2 imply that interactions of one sample molecule with several C_{18} ligands are impossible and that all C_{18} ligands do not necessarily contribute to the retention behavior of the sample molecule, even at high values of $\sigma_{C_{18}}$. This suggests also that sample molecules, at least those as small as the benzene derivatives used in this study, interact probably with only one C_{18} ligand at low $\sigma_{C_{18}}$. In addition, the solid and the dashed straight lines tend to pass close to the origin. In Eq. (4), the intercept (β') should be equal to zero because the retention of the sample molecules on the C_{18} ligands originates from hydrophobic interactions. No hydropho-

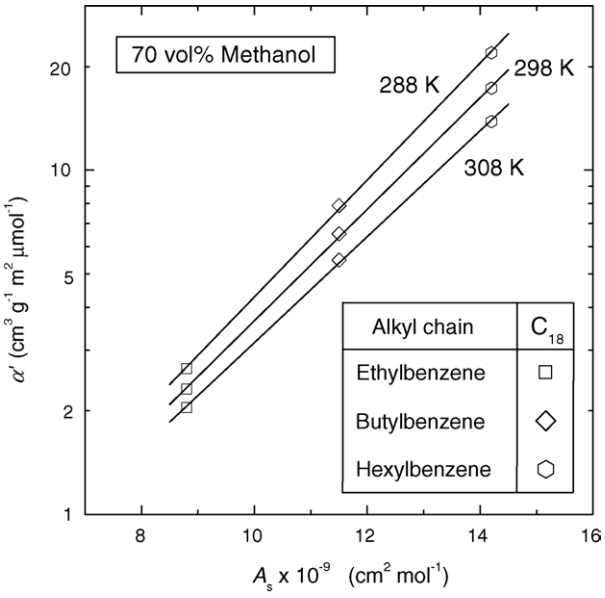

Fig. 3. Logarithm of α' as a function of A_s of the sample molecules.

bic interaction takes place when there is no C_{18} ligand on the stationary phase surface.

Fig. 3 shows a plot of $\log \alpha'$ versus the hydrophobic surface area of the sample molecules (A_s), a measure of the molecular size calculated as the sum of the surface area increments for each group of the molecule [34]. The relationship is linear. The ratio of the α' values for two compounds represents the difference in their retention strength, for instance K, on the C_{18} ligands under the condition that one sample molecule interacts with a single C_{18} ligand. The slope of the straight line in Fig. 3 is 3.7×10^{-6} m^3 mol-C_{18}-ligand g^{-1} mol^{-1} sample molecule. This means that the retention strength of the alkylbenzene derivatives increases by a factor of about 1.7 for the addition of one methylene unit to the sample molecule.

The solvophobic theory [18,35,36] assumes that the retention of sample molecules on alkyl ligands in RPLC results from the decrease in the contact area between the polar mobile phase solvent and the hydrophobic surfaces of both the sample molecule and the alkyl ligand that takes place upon adsorption of a sample molecule. The reduction of the hydrophobic surface area (ΔA) is assumed to be a fraction of A_s. As the result of adequate modifications, the difference in $\log K$ two homologous compounds, i and j, is represented as follows [18,35].

$$\ln K_i - \ln K_j = \frac{N_A \gamma \alpha (A_{s,i} - A_{s,j})}{RT} \quad (5)$$

where N_A is the Avogadro number, γ the surface tension of the mobile phase solvent, α the ratio of ΔA to A_s, R the gas constant, and T the absolute temperature. The value of α depends on some chromatographic conditions such as the type and composition of the organic modifier in the mobile phase and the length of the alkyl ligands bonded to the stationary phase surface in RPLC [18]. For instance, the value of α has been reported as about 0.30–0.35 for the RPLC system made of the C_{18}-silica gel #5 and a methanol/water mixture (70/30, v/v) [18]. Similar values of α were also reported for the RPLC system made of a C_{18}-silica gel and an aqueous buffer as the mobile phase ($\alpha = 0.35$) [35] and for the system of an activated carbon and water ($\alpha = 0.2$–0.3) [36]. Eq. (5) indicates that the increment in $\log K$ due to the addition of one methylene unit to the sample molecule is about 1.7 under the RPLC conditions of this study, if we assume $\alpha = 0.35$. This value agrees well with that derived from Fig. 3. The results in Figs. 2 and 3 suggest that the retention behavior on the C_{18}-silica gels with different densities of C_{18} and C_1 ligands is well accounted for by adding the contributions of the two alkyl ligands.

Enthalpy–entropy compensation of retention equilibrium. The goal of this study is to characterize more clearly, from the thermodynamic and the extrathermodynamic viewpoints, retention equilibria in RPLC. This work is done using a series of silica gels bonded with C_{18} and C_1 ligands, with different chain densities, i.e., a series of fully end-capped C_{18}-silicas with variable density of the alkyl chain. Fig. 1 shows that the carbon content of the adsorbent is a primary parameter, which roughly represents the amount of alkyl ligands bonded to the surface of the base silica gel. However, this parameter depends on both the density and the length of the alkyl ligands. Additionally, the ligand density of a given packing material depends on the length of the main alkyl chains, even if we use the same base silica gel to prepare it. So, the retention data on silica gels bonded with different amounts of different alkyl ligands cannot be directly compared. The experimental data should be analyzed based on the retention equilibrium parameter normalized by the ligand density. As indicated in Figs. 2 and 3, the retention behavior on the C_{18}-silica gels having different densities of C_{18} and C_1 ligands is explained by assuming that the contributions of the C_{18} and C_1 ligands to retention are additive and that each contribution is proportional to the density (σ) of the corresponding alkyl ligand. We introduce a hypothetical value of the retention equilibrium constant (κ), which would be measured by using silica gel particles chemically modified with an alkyl ligand of unit density. The value of κ is calculated as the ratio of K to σ. We analyzed the experimental values of κ, rather than K.

The temperature dependence of κ was analyzed according to the following equation

$$\ln \kappa = -\frac{\Delta H}{RT} + \frac{\Delta S}{R} \quad (6)$$

where ΔH and ΔS are the enthalpy and the entropy changes of the retention, respectively. The conventional procedure consists in (1) calculating ΔH and ΔS from the slope and the intercept of the linear plot of $\ln \kappa$ versus $1/T$; (2) confirming a linear correlation between ΔH and ΔS and assuming the existence of an EEC; and (3) deriving T_c from the slope of the linear correlation between ΔH and ΔS. However, Krug et al. [21–23] criticized this procedure harshly, claiming that (1) a linear correlation can be observed between ΔH and ΔS even when no true EEC takes place; (2) this apparent EEC originates from compensation between errors made in the determination of the two thermodynamic parameters based on the linear regression of the van't Hoff plot; and (3) in the case of a merely appar-

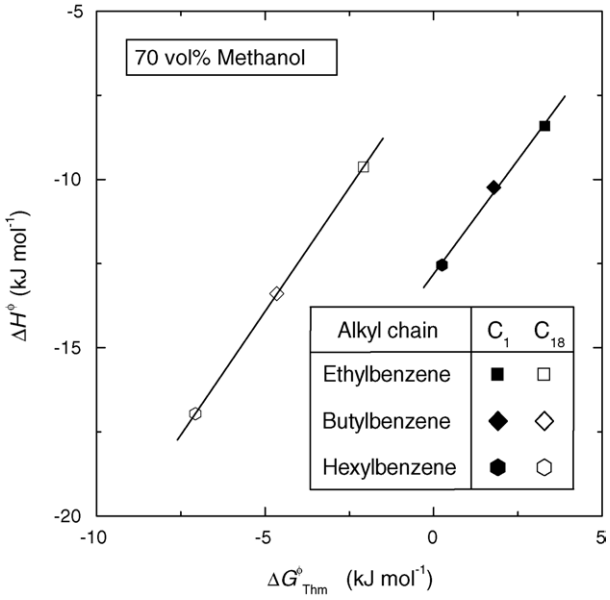

Fig. 4. Plot of ΔH^{Φ} against $\Delta G^{\Phi}_{T_{hm}}$.

ent EEC, the slope and the correlation coefficient of the linear correlation between ΔH and ΔS are respectively equal to the harmonic mean temperature (T_{hm}) and close to unity. They proposed four different methods to ascertain whether the linear correlation between ΔH and ΔS is based on substantial physico-chemical effects or results merely from a statistical compensation due to experimental errors [21–23]. We checked our experimental retention data using all four tests proposed by Krug et al. to verify that there is a true EEC effect. In the following, we describe only the results of these tests. Detailed information about the Krug's four approaches can be found in other literature [21–23].

3.1. Plot of ΔH^{Φ} versus $\Delta G^{\Phi}_{T_{hm}}$

Krug et al. recommended that $\ln \kappa$ be plotted against $\{1/T - \langle 1/T \rangle\}$, rather than $1/T$, to obtain more accurate values of related thermodynamic parameters, i.e., ΔH^{Φ} and the Gibbs free energy change due to the sample retention at $T_{hm}(\Delta G^{\Phi}_{T_{hm}})$ The brackets ($\langle\rangle$) and superscript Φ denote an average value and the thermodynamic parameters derived from the plot between $\ln \kappa$ and $\{1/T - \langle 1/T \rangle\}$, respecitvely. Krug et al. claimed that a linear correlation should be observed between ΔH^{Φ} and $\Delta G^{\Phi}_{T_{hm}}$ when a real EEC takes place. Fig. 4 shows a linear correlation between ΔH^{Φ} and $\Delta G^{\Phi}_{T_{hm}}$. The compensation temperatures (T_c^{Φ}) are derived from the slope of the linear plots between $\ln \kappa$ and $\{1/T - \langle 1/T \rangle\}$ as 930 and 1140 K for the sample retention on C_{18} and C_1 ligands, respectively. These values are of the same order of magnitude as those previously reported for retention equilibria in RPLC systems [10,11,17–20].

3.2. Comparison of T_c^{Φ} with T_{hm} (hypothesis test)

Krug et al. claimed that T_c^{Φ} should be significantly different from T_{hm} (=298 K) and that the null hypothesis, $T_c^{\Phi} = T_{hm}$, is rejected when substantial compensation effects take place [21]. Table 2 lists the calculated values of T_c^{Φ} (minimum) and T_c^{Φ} (maximum). The hypothesis can be rejected for the retention equilibrium in RPLC, although the confidence level for the C_1 ligand is rather low.

Table 2
Compensation temperatures of the retention equilibrium

	T_c^{Φ} (K)[a]	T_c^{Φ} (K)[b]		Confidence level $(1-\alpha_s)\times 100\%$
		Minimum	Maximum	
C_1 ligand	1.1×10^3	5.0×10^2	1.7×10^3	>80
C_{18} ligand	9.3×10^2	5.4×10^2	1.3×10^3	>99

[a] T_c^{Φ} calculated from the slope of the linear correlation between ΔH^{Φ} and $\Delta G^{\Phi}_{T_{hm}}$ in Fig. 4.
[b] Range of T_c^{Φ} at $(1-\alpha_s) \times 100\%$ confidence level calculated by the estimation method proposed by Krug et al. [21].

3.3. Convergence of the van't Hoff plots at T_c^{Φ}

Fig. 5a and b shows the van't Hoff plot of κ_{C_1} and $\kappa^0_{C_{18}}$, respectively. The value of κ_{C_1} is the ratio of K_{C_1} calculated by Eq. (3) to σ_{C_1}. Similarly, $\kappa_{C_{18}}$ is calculated by dividing K_{C18} by $\sigma_{C_{18}}$. As shown in Fig. 2, however, $\kappa_{C_{18}}$ decreases with increasing $\sigma_{C_{18}}$. We used the value of $\kappa^0_{C_{18}}$ at low $\sigma_{C_{18}}$ because $\kappa^0_{C_{18}}$ is independent of $\sigma_{C_{18}}$ and because, as indicated earlier, a sample molecule interacts with only one C_{18} ligand in the low $\sigma_{C_{18}}$ range. The superscript 0 refers to the slope of the linear regression of the plots for the C_{18}-silica gels #1–#3 in Fig. 2. Consequently, $\kappa^0_{C_{18}}$ is equal to α' as indicated in Eq. (4). The linear van't Hoff plots properly intersect in a small region of the plane, suggesting that almost the same values of κ would be observed around the intersection point, irrespective of the compound used. Additionally, the T_c values estimated from the intersection point in Fig. 5a and b are properly close to those of T_c^{Φ} estimated from the slope of the linear correlations between ΔH^{Φ} and $\Delta G^{\Phi}_{T_{hm}}$ in Fig. 4.

3.4. Probability for the intersection of the van't Hoff plots

According to the F-test, the probability for the intersection of the van't Hoff plots in Fig. 5a and b was compared with that for a nonintersection, on the basis of the statistical data derived by an analysis of variance (ANOVA) procedure [23]. The probability for nonintersection was also compared to the precision of the experimental data in the same manner. Table 3 lists the values of the mean sum of squares (MS) calculated. The MS value for the intersection (MS_{con}) is more than two orders of magnitude larger than that for nonintersection (MS_{noncon}). The ratio MS_{con}/MS_{noncon} for the C_1 ligand is sufficiently larger than the F-value, $F(1, 1, 1-\alpha_s = 0.95) = 161$. Although the ratio for the C_{18} ligand is slightly smaller than the F-value, they are close. This shows that the probability for intersection is high compared to that for nonintersection in both cases. On the other hand, the ratio of MS_{noncon} to the mean sum of squares of the residuals (MS_ε) is sufficiently smaller than the corresponding F-value, $F(1, 2, 1-\alpha_s = 0.95) = 18.5$, although the values of MS_{noncon}

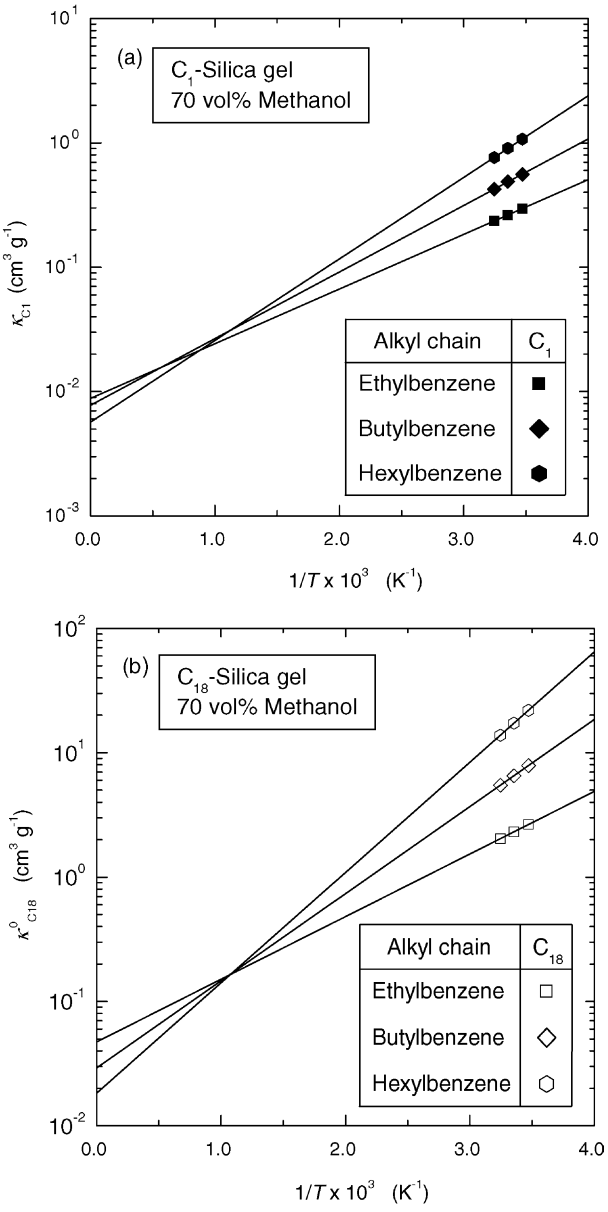

Fig. 5. Temperature dependence of (a) κ_{C_1} and (b) $\kappa^0_{C_{18}}$.

and MS_ε are of the same order of magnitude. The negative value of MS_ε in the case of the C_1 ligand is probably unreasonable. However, it seems to arise from calculation errors, which suggests that the variation due to measurement errors is quite small. In conclusion, the variation due to nonconcurrence is not greater than that due to the measurement errors at the $100\alpha_s$% level of significance.

On the basis of the results described above, we can state that a true EEC takes place for retention equilibria, originating from substantial physico-chemical effects. The retention mechanism seems to be similar, irrespective of the sample compound in RPLC systems using either the C_1 or the C_{18} alkyl chain bonded silica gel.

Linear free energy relationships of retention equilibrium. Linear free energy relationships (LFER) as well as EEC are used to study the mechanisms of equilibria or kinetic processes. In RPLC, LFER correlations are also observed between different retention equilibria and/or mass transfer kinetics. The free energy change (ΔG) associated with a retention equilibrium is linearly correlated with that under different RPLC conditions and even with a related kinetic process, e.g., surface diffusion [18,33].

3.5. Influence of the change in RPLC conditions on the retention equilibrium

Fig. 6a shows the temperature dependence of κ_{C_1}. Only the column temperature was changed. The values of κ_{C_1} at 288 and 308 K (symbols) are linearly correlated with those at 298 K (straight line), suggesting the presence of a LFER between κ_{C_1} values at the two temperatures. The slope of the linear correlation at 288 K is slightly larger than that at 308 K. Similar results are observed for the temperature dependence of $\kappa^0_{C_{18}}$ in Fig. 6b.

In Fig. 7, the values of κ_{C_1} at the same three temperatures are plotted against that of $\kappa^0_{C_{18}}$ at 298 K. In this case, both the chain length of the alkyl ligands bonded onto the stationary phases and the temperature were simultaneously changed. Again, a LFER takes place between the retention equilibria under the different RPLC conditions.

Table 3
ANOVA table of the retention equilibrium on the different alkyl ligands

Source of variation	DF[a]	SS[b]	MS[c]	C_1 ligand ($p=3$[d], $q=3$[e])			C_{18} ligand $p=3$[d], $q=3$[e])		
				DF[a]	SS[b]	MS[c]	DF[a]	SS[b]	MS[c]
Total	$pq-1$	SS_T	MS_T	8	2.4	3.0×10^{-1}	8	7.1	8.8×10^{-1}
Rows (samples)	$p-1$	SS_R	MS_R	2	2.3	1.1×10^{-1}	2	6.9	3.4
Columns (temperatures)	$q-1$	SS_C	MS_C	2	1.2×10^{-1}	6.0×10^{-2}	2	2.0×10^{-1}	9.9×10^{-2}
Interactions	$(p-1)(q-1)$	SS_{RC}	MS_{RC}	4	3.1×10^{-3}	7.7×10^{-4}	4	1.2×10^{-2}	2.9×10^{-3}
Slope	$p-1$	SS_S	MS_S	2	3.2×10^{-3}	1.6×10^{-3}	2	1.2×10^{-2}	5.8×10^{-3}
Concurrence	1	SS_{con}	MS_{con}	1	3.1×10^{-3}	3.1×10^{-3}	1	1.1×10^{-2}	1.1×10^{-2}
Nonconcurrence	$p-2$	SS_{noncon}	MS_{noncon}	1	1.2×10^{-5}	1.2×10^{-5}	1	9.6×10^{-5}	9.6×10^{-5}
Residuals	$(p-1)(q-2)$	SS_ε	MS_ε	2	-9.1×10^{-5}	-4.6×10^{-5}	2	1.2×10^{-4}	6.1×10^{-5}

[a] DF is the degree of freedom.
[b] SS is the sum of squares.
[c] MS is the mean sum of squares, MS = SS/DF, for each source of variation.
[d] p is the number of the sample compounds.
[e] q is the number of experimental temperatures.

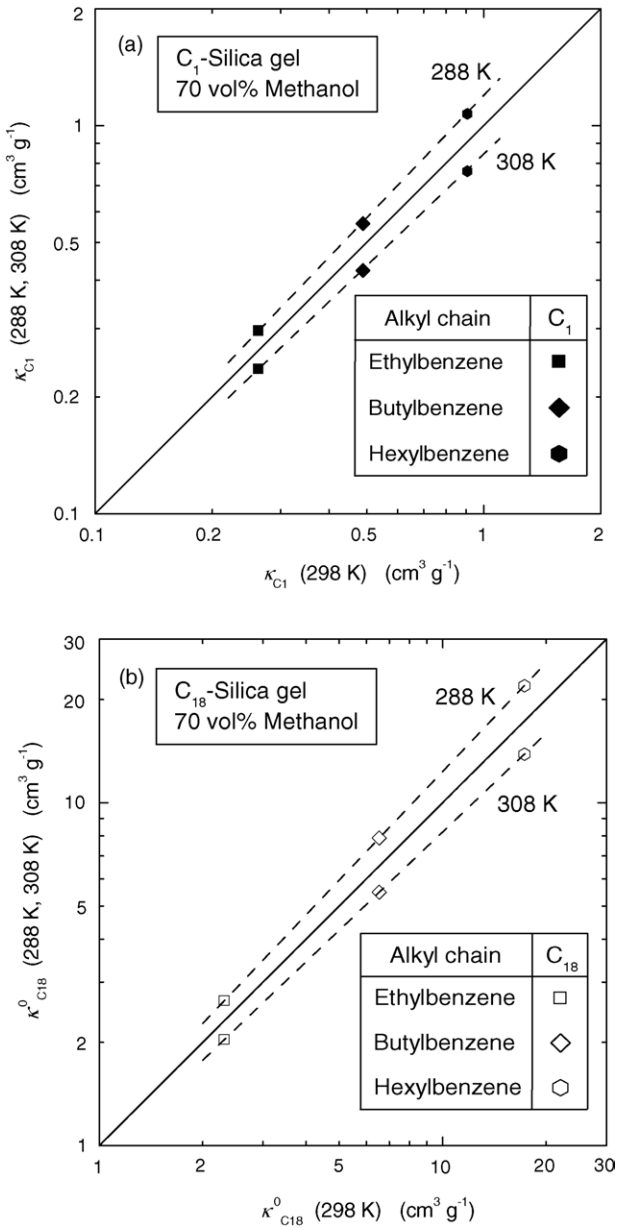

Fig. 6. Correlation between (a) κ_{C_1} and (b) $\kappa^0_{C_{18}}$ values at different temperature conditions.

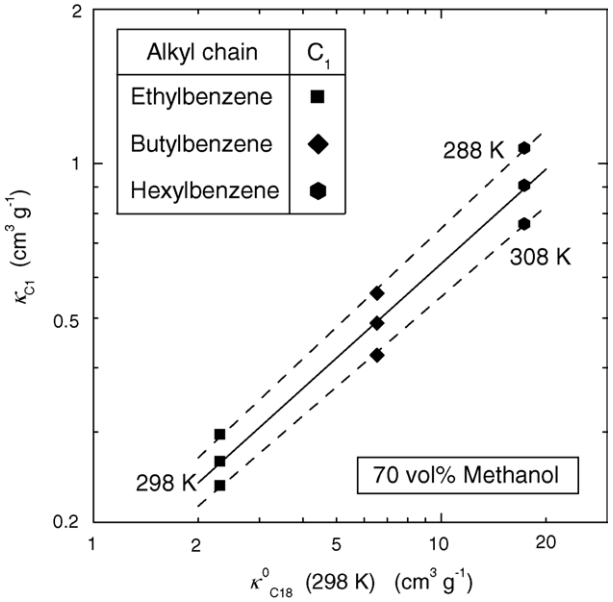

Fig. 7. Correlation between κ_{C_1} and $\kappa^0_{C_{18}}$ values at different temperature conditions.

3.6. A model for explaining the change of the retention behavior

As shown in Figs. 6 and 7, the retention behavior in RPLC depends on some experimental parameters. In the following, a model based on an EEC and a LFER was developed by assuming that the ΔG value of the retention equilibrium consists of the sums of incremental contributions due to the structural elements of molecules. The retention behavior in RPLC and its thermodynamic properties were studied from the viewpoints of the molecular structural contributions by analyzing the two extrathermodynamic correlations. This model provides a comprehensive explanation of the variation of K due to changes in the RPLC conditions.

The free energy change of retention (ΔG^{Φ}) is related to κ as follows:

$$\Delta G^{\Phi^{\mathrm{REF}}}_{T_1} = -RT_1 \ln \kappa^{\mathrm{REF}}_{T_1} \tag{7}$$

$$\Delta G^{\Phi^{\mathrm{SMP}}}_{T_2} = -RT_2 \ln \kappa^{\mathrm{SMP}}_{T_2} \tag{8}$$

where T_1 and T_2 stand for the column temperatures and the superscripts REF and SMP denote the reference and the sample systems, respectively. The value of $\log \kappa^{\mathrm{SMP}}_{T_2}$ is linearly correlated with $\log \kappa^{\mathrm{REF}}_{T_1}$, as illustrated in Figs. 6 and 7, suggesting a LFER of the retention equilibrium between the corresponding RPLC systems.

$$\ln \kappa^{\mathrm{SMP}}_{T_2} = A \ln \kappa^{\mathrm{REF}}_{T_1} + B \tag{9}$$

Substituting Eqs. (7) and (8) into Eq. (9) gives

$$\Delta G^{\Phi^{\mathrm{SMP}}}_{T_2} = A \left(\frac{T_2}{T_1} \right) \Delta G^{\Phi^{\mathrm{REF}}}_{T_1} - RT_2 B \tag{10}$$

Eq. (10) formulates the LFER of retention behavior between different RPLC conditions.

On the other hand, ΔG^{Φ} consists of the contributions of an enthalpy (ΔH^{Φ}) and an entropy change (ΔS^{Φ}), according to the Gibbs–Helmholtz relation.

$$\Delta G^{\Phi} = \Delta H^{\Phi} - T\Delta S^{\Phi} \tag{11}$$

It is assumed that ΔG^{Φ} of a molecule involved in hydrophobic interactions is correlated with a parameter describing a molecular property (X_{m}) [25,37].

$$\Delta G^{\Phi} = a_{\mathrm{g}} X_{\mathrm{m}} + b_{\mathrm{g}} \tag{12}$$

where a_{g} and b_g are molecular thermodynamic parameters. The value of a_{g} is ΔG^{Φ} per unit value of the molecular property X_{m} and that of b_{g} is ΔG^{Φ} at $X_{\mathrm{m}} = 0$. Various molecular properties

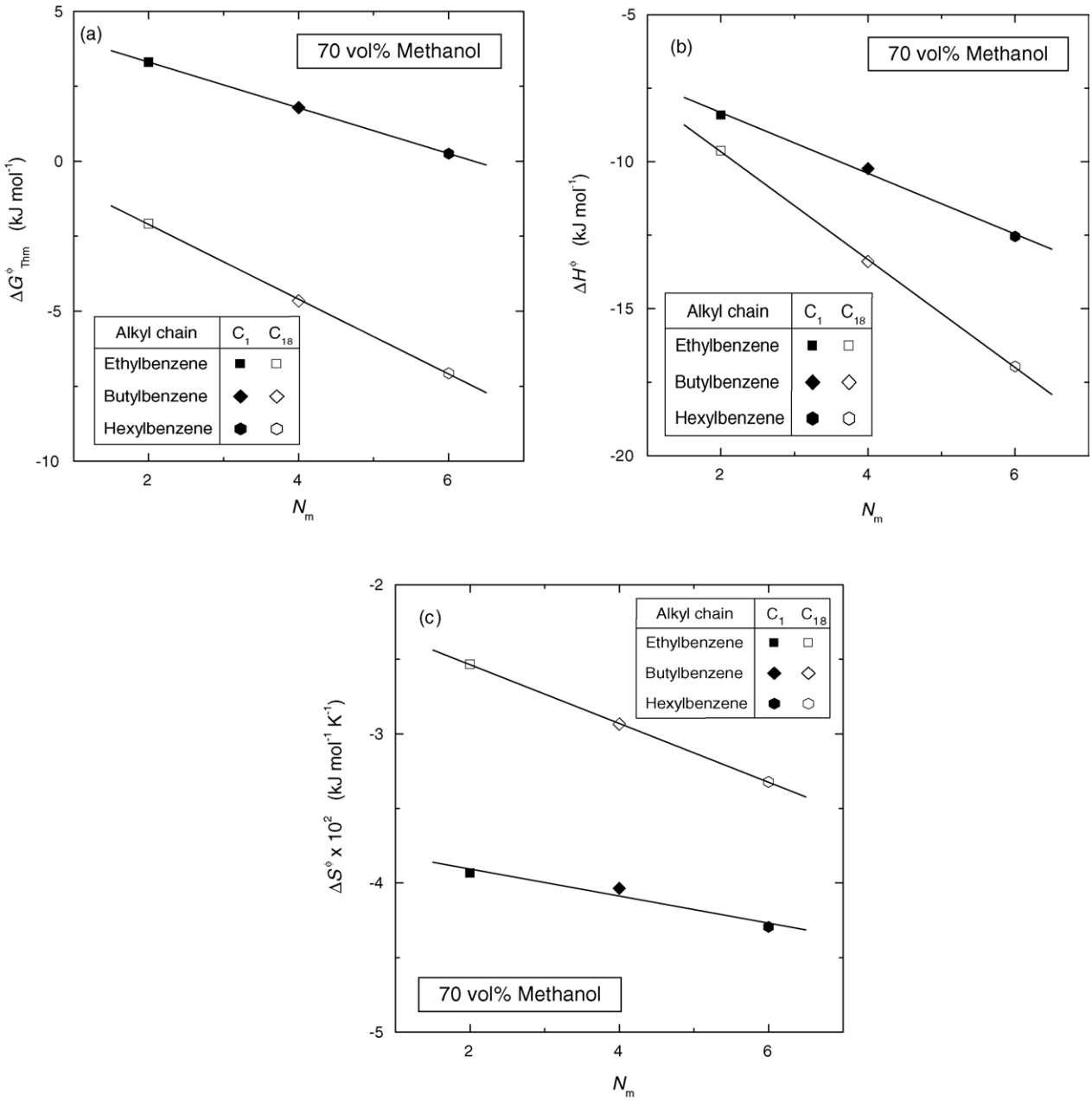

Fig. 8. Correlations between (a) $\Delta G^{\Phi}_{T_{hm}}$ and N_m, (b) ΔH^{Φ} and N_m, and (c) ΔS^{Φ} and N_m.

can be taken for X_m, for instance, the surface area of the nonpolar part of the molecule or the number of recurring structural elements. In this study, we used alkylbenzene derivatives as the sample compounds. The number of methylene group (N_m) in the alkyl chain of the molecules was used as X_m. Fig. 8a shows the linear correlations of ΔG^{Φ} at T_{hm} (298 K) with N_m for both the C_1- and C_{18}-silica gels. The results in Fig. 8a demonstrate the validity of Eq. (12).

It is expected that ΔH^{Φ} and ΔS^{Φ} are similarly represented using the corresponding molecular thermodynamic parameters (a_h, b_h, a_s, and b_s) as follows [25,37].

$$\Delta H^{\Phi} = a_h X_m + b_h \quad (13)$$

$$\Delta S^{\Phi} = a_s X_m + b_s \quad (14)$$

Fig. 8b shows the plots of ΔH^{Φ} against N_m. Linear correlations are observed between ΔH^{Φ} and N_m. Fig. 8c similarly shows ΔS^{Φ} as a function of N_m. Again, ΔS^{Φ} is linearly correlated with N_m. The results in Fig. 8b and c suggests the validity of Eqs. (13) and (14). Table 4 lists the resulting values of the slope (a) and the intercept (b). Using the slopes of the straight lines between ΔH^{Φ} and $N_m(a_h)$ and between ΔS^{Φ} and $N_m(a_s)$, T_c^{Φ} can be calculated as [25].

$$T_c^{\Phi} = \frac{a_h}{a_s} \quad (15)$$

Table 4 also lists the ratios of a_h to a_s, in fairly good agreement with those of T_c^{Φ} in Table 2.

Table 4
Molecular thermodynamic parameters

	ΔH^{Φ} vs. N_m		ΔS^{Φ} vs. N_m		T_c^{Φ} (=a_h/a_s) (K)
	a_h (kJ mol^{-1})	b_h (kJ mol^{-1})	a_s (kJ mol^{-1} K^{-1})	b_s (kJ mol^{-1} K^{-1})	
C_1 ligand	−1.0	−6.3	-9.1×10^{-4}	-3.7×10^{-2}	1.1×10^3
C_{18} ligand	−1.8	−6.0	-2.0×10^{-3}	-2.1×10^{-2}	9.3×10^2

Differentiation of both sides of Eq. (10) with respect of N_m gives

$$\frac{\partial \Delta G_{T_2}^{\Phi^{SMP}}}{\partial N_m} = A\left(\frac{T_2}{T_1}\right)\frac{\partial \Delta G_{T_1}^{\Phi^{REF}}}{\partial N_m} \quad (16)$$

The following equation is derived from a combination of Eqs. (11), (13), and (14).

$$\Delta G^{\Phi} = \Delta H^{\Phi} - T\Delta S^{\Phi} = (a_h N_m + b_h) - T(a_s N_m + b_s) \quad (17)$$

Substituting Eqs. (17) and (16) and rearranging gives

$$A = \frac{a_s^{SMP} T_1 (T_c^{\Phi^{SMP}} - T_2)}{a_s^{REF} T_2 (T_c^{\Phi^{REF}} - T_1)} \quad (18)$$

where a_s^{REF} and a_s^{SMP} are the increments of ΔS^{Φ} corresponding to the addition of one methylene unit to the alkyl chain of the sample molecule, in the reference and the sample systems, respectively. Eq. (18) shows that A depends on the temperature and that this temperature dependence is correlated with T_1, T_2, $T_c^{\Phi^{REF}}$, and $T_c^{\Phi^{SMP}}$.

On the other hand, substituting Eqs. (17)–(10) gives B (Eq. (9)), as follows.

$$B = \frac{1}{RT_2}\left[A\left(\frac{T_2}{T_1}\right)(b_h^{REF} - T_1 b_s^{REF}) - (b_h^{SMP} - T_2 b_s^{SMP})\right] \quad (19)$$

Eqs. (18) and (19) shows the dependence of the slope and the intercept of the LFER in Eq. (10) on the molecular thermodynamic parameters (a and b) in Eqs. (13) and (14), the compensation temperatures (T_c^{Φ}), and experimental temperature (T).

3.7. Interpretation of the variations of κ on the basis of the EEC

It is expected that Eqs. (18) and (19) can explain effectively the variation of κ arising from changes in the RPLC conditions. When only the temperature is changed, Eqs. (18) and (19) should be modified as follows.

$$A = \frac{T_1(T_c^{\Phi} - T_2)}{T_2(T_c^{\Phi} - T_1)} \quad (20)$$

$$B = \frac{1}{RT_2}\left[A\left(\frac{T_2}{T_1}\right)(b_h - T_1 b_s) - (b_h - T_2 b_s)\right] \quad (21)$$

The dashed lines in Figs. 6a and b were calculated with Eqs. (20) and (21), taking T_1 = 298 and T_2 = 288 or 308 K. The experimental data points lay close to the corresponding straight lines, demonstrating the validity of the model developed for explaining the temperature dependence of κ (hence of K).

When the temperature is constant, Eqs. (18) and (19) become

$$A = \frac{a_s^{SMP}(T_c^{\Phi^{SMP}} - T)}{a_s^{REF}(T_c^{\Phi^{REF}} - T)} \quad (22)$$

$$B = \frac{1}{RT}[A(b_h^{REF} - Tb_s^{REF}) - (b_h^{SMP} - Tb_s^{SMP})] \quad (23)$$

The solid line in Fig. 7 was calculated with Eqs. (22) and (23), at constant temperature (298 K). The two dashed lines in Fig. 7 were similarly calculated with Eqs. (18) and (19) because, in that case, both the type of alkyl ligand (C_1 or C_{18}) and the temperature were simultaneously changed. Again, all the experimental data properly overlay the corresponding straight lines. The results in Figs. 6 and 7 demonstrate that Eqs. (18) and (19) are useful to analyze the variation of the retention equilibrium (i.e., κ and K) due to changes of the RPLC experimental conditions on the basis of the EEC and of molecular thermodynamic contributions.

3.8. Estimation of the value of K

The results described above suggest that it should be possible to estimate the value of κ, hence K, under various RPLC conditions, from a limited number of experimental data of K. In the following, we calculate K for the three sample compounds (ethyl-, n-butyl-, and n-hexyl-benzene) between 288 and 308 K, on the RPLC packing materials #1–#6 bonded with C_{18} and C_1 ligands at different densities, with a methanol/water (70/30, v/v) solution, from only one experimental datum, K of n-hexylbenzene at 298 K on the C_{18}-silica gel #5, using Eqs. (18) and (19) based on the EEC and LFER, assuming the additivity of the contributions of the C_{18} and the C_1 ligands to the retention constant. In this problem, four RPLC conditions are simultaneously changed, the sample compound, the composition of the bonded layer (C_1 and C_{18}), the density of the alkyl ligands, and the column temperature. First, the values of κ_{C_1} and $\kappa_{C_{18}}$ of the three sample compounds are calculated at the three different temperatures from the value of $\kappa_{C_{18}}$ for n-hexylbenzene at 298 K using Eqs. (18) and (19), the molecular thermodynamic parameters a and b listed in Table 4, and the compensation temperatures (T_c^{Φ}) listed in Tables 2 and 4. The primary value of $\kappa_{C_{18}}$ of n-hexylbenzene at 298 K was simply calculated as the ratio of the experimental value of K on the C_{18}-silica gel #5 to its C_{18} ligand density ($\sigma_{C_{18}}$). Then, the values of K on the other silica gels (#1–#6) were calculated as the sums of the contributions of the two alkyl ligands to the retention constant. The multiplication of

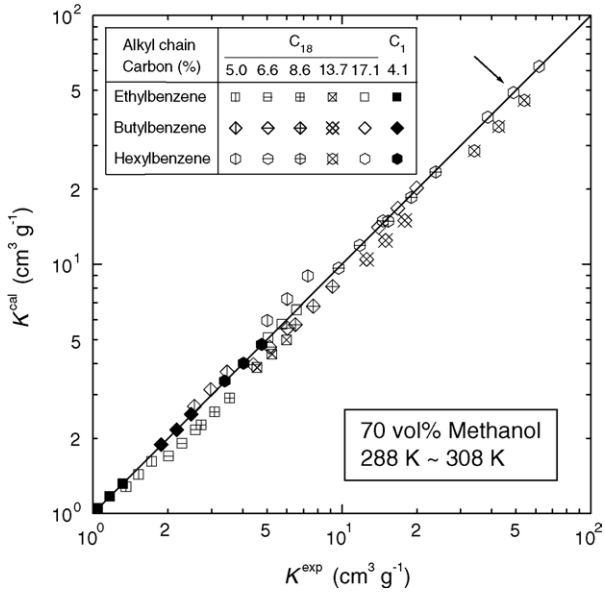

Fig. 9. Comparison of K^{exp} with K^{cal} estimated from only one experimental datum of K of *n*-hexylbenzene on the C_{18}-silica gel #5 at 298 K.

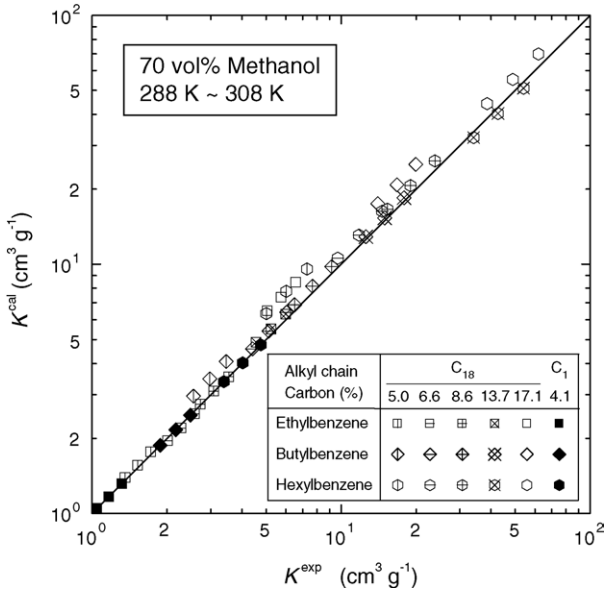

Fig. 10. Comparison of K^{exp} with K^{cal} estimated from α' ($=\kappa^0_{C_{18}}$) of *n*-hexylbenzene at 298 K.

$\kappa_{C_{18}}$ by $\sigma_{C_{18}}$ gives the contribution of the C_{18} ligand bonded on the stationary phase surface to the sample retention. The contribution of the C_1 ligand was calculated in the same way. Finally, the contributions of the two alkyl ligands were added to derive the K values.

Fig. 9 compares K so calculated (K^{cal}) with the experimental data (K^{exp}). The arrow in Fig. 9 indicates the original datum of K experimentally measured, from which all the values of K^{cal} in Fig. 9 were estimated under the different RPLC conditions. All the data points lay on or scatter around the diagonal line having the slope unity, proving the validity of our model of retention equilibrium based on the EEC and the assumption that the contributions of the C_1 and the C_{18} ligands to the sample retention are additive and that the contributions of the two alkyl ligands are calculated as the product of κ and σ. We calculated the mean square deviation (MSD) according to the following equation (Eq. (24)).

$$\mathrm{MSD} = \left[\left(\frac{1}{N}\right)\sum\left[\frac{K^{cal} - K^{exp}}{K^{exp}}\right]^2\right]^{1/2} \quad (24)$$

where N is the number of data pairs of (K^{exp} and K^{cal}). The value of MSD was calculated as 0.11 for the results in Fig. 9. Our model (Eqs. (18) and (19)) provides a comprehensive explanation of the intrinsic characteristics of the retention equilibrium in RPLC from the viewpoints of thermodynamics and extrathermodynamics.

However, the results in Fig. 2 suggests that the $\kappa_{C_{18}}$ value ($= K^{exp}_{(\#5)}/\sigma_{C_{18}}$) used in the calculations described above is not equal to $\kappa^0_{C_{18}}$, which is calculated from the slope of the linear line in the range of small σ_{C18} values in Fig. 2. The value of $\kappa_{C_{18}}$ should be smaller than κ^0_{C18}. As a result, many values of K^{cal} in Fig. 9 are slightly below the diagonal line. Accordingly, we recalculated the same set of K^{cal} values but used instead the values of α' ($=\kappa^0_{C_{18}}$) in Fig. 3 as $\kappa_{C_{18}}$. The new values of κ_{C1} for the sample compounds were calculated as the ratio of K^{exp}_{TMS} at each temperature to σ_{C_1}. Then, K^{cal} was derived in the same manner as described above. The values of K^{cal} are compared with K^{exp} in Fig. 10. Again, all the data points scatter around the diagonal line. The value of MSD for Fig. 10 was similarly calculated as 0.13, which is almost the same as that for Fig. 9. The K^{cal} values in Fig. 10 are slightly larger compared to the corresponding ones in Fig. 9. This difference comes probably from the difference between the α' values (Eq. (4)) used for calculating K^{cal} in Figs. 9 and 10. For Fig. 9, the α' values under different RPLC conditions were estimated from only one source, the value of $\kappa_{C_{18}}$ of *n*-hexyl-benzene at 298 K, by applying the new EEC model for retention (Eqs. (18) and (19)) with the related parameters (a, b, and T_c^{Φ}) listed in Tables 2 and 4. The original κ_{C18} value was the ratio of K^{exp} at 298 K to $\sigma_{C_{18}}$ of the C_{18}-silica gel #5. On the other hand, $\kappa^0_{C_{18}}$ was used as α' in the case of Fig. 10. As shown in Fig. 2, the value of $K^0_{C_{18}}$ is larger than the ratio of K^{exp} to $\sigma_{C_{18}}$ (C_{18}-silica gel #5) for each sample compound. Ultimately, yet, the results in Figs. 9 and 10 prove the validity of our model of the retention equilibrium based on the EEC.

4. Conclusion

Two extrathermodynamic relationships, i.e., EEC and LFER, relate the retention equilibrium data in RPLC systems made of silica gels bonded with mixtures of C_1 and C_{18} alkyl ligands at different densities. Assuming that the contributions of the C_1 and the C_{18} ligands to retention are additive and that the contribution of each ligands can be calculated as the product of a normalized adsorption constant, κ, and the ligand density, σ, we demonstrated first that the EEC of the retention equilibrium is true and that it is based on substantial physico-chemical effects.

This is the result of the analysis of the modified van't Hoff plot and of the four tests proposed by Krug et al. The values of T_c^{Φ} were estimated at about 1.1×10^3 K and 9.3×10^2 K for the C_1 and C_{18} ligands, respectively.

Then, a new model based on the EEC so demonstrated was derived to explain the LFER of the retention equilibrium under different RPLC conditions. The values of the changes in free energy, $\Delta G^{\Phi}_{T_{hm}}$, enthalpy, ΔH^{Φ}, and entropy, ΔS^{Φ} are linearly correlated with the numbers of methylene groups, N_m. The ratio of the slopes a_h to a_s was found to be close to the compensation temperature, T_c^{Φ}, calculated from the slope of the linear correlation between ΔH^{Φ} and $\Delta G^{\Phi}_{T_{hm}}$. The slope (A) and the intercept (B) of the LFER between the values of κ under different RPLC conditions are accounted for by T_c^{Φ}, a, and b.

Finally, the model allows an accurate prediction of the K values under different RPLC conditions from only one experimental datum with the MSD of 0.11, regardless of the simultaneous change of four RPLC conditions, i.e., the sample compound, the composition of the bonded layer (C_1 and C_{18}), the density of the alkyl ligands, and the column temperature. This new model (Eqs. (18) and (19)) provides a comprehensive explanation of the intrinsic characteristics of the retention equilibrium in RPLC from the viewpoints of thermodynamics and extrathermodynamics.

5. Nomenclature

a	slope of the linear correlation between a thermodynamic property and X_m
A	slope of LFER (Eq. (9))
A_s	hydrophobic surface area of the sample compound ($cm^2\,mol^{-1}$)
ΔA	reduction of total hydrophobic surface area due to sample retention ($cm^2\,mol^{-1}$)
b	intercept of the linear correlation between a thermodynamic property and X_m
B	intercept of LFER (Eq. (9))
C	carbon content of the packing materials (wt.%)
ΔG	free energy change ($kJ\,mol^{-1}$)
ΔH	enthalpy change ($kJ\,mol^{-1}$)
κ'	retention factor
K	retention equilibrium constant ($cm^3\,g^{-1}$)
L	column length (mm)
MS	mean sum of squares
MSD	mean square deviation
N	number of data pairs of (K^{exp} and K^{cal})
N_A	Avogadro number (mol^{-1})
N_m	number of methylene group
R	gas constant ($J\,mol^{-1}\,K^{-1}$)
ΔS	entropy change ($kJ\,mol^{-1}\,K^{-1}$)
SS	sum of squares
T	absolute temperature (K)
T_c	compensation temperature (K)
T_{hm}	harmonic mean of experimental temperatures (K)
u_0	superficial velocity ($cm\,s^{-1}$)
X_m	property of molecule

Greek letters

α	ratio of ΔA to A_s in Eq. (5)
α_s	statistical level of significance
α_{sep}	separation factor
α'	coefficient in Eq. (4) ($cm^3\,g^{-1}\,m^2\,\mu mol^{-1}$)
β'	coefficient in Eq. (4) ($cm^3\,g^{-1}$)
ε_e	void fraction of the column
ε_p	porosity of the stationary phase particle
κ	K value normalized by σ ($cm^3\,g^{-1}$)
μ_1	first absolute moment (s)
ρ_p	particle density ($g\,cm^{-3}$)
σ	alkyl ligand density ($\mu mol\,m^{-2}$)

Superscripts

cal	calculated
exp	experimental
REF	reference
SMP	sample
0	equilibrium parameter determined from the experimental retention data in the range of low $\sigma_{C_{18}}$
Φ	thermodynamic parameters measured by analyzing temperature dependence of κ

Subscripts

con	concurrence
C_1	contribution of C_1 ligand
C_{18}	contribution of C_{18} ligand
g	free energy change
h	enthalpy change
i	ith component
j	jth component
noncon	nonconcurrence
ODS	experimental data measured using the C_{18}-silica gel column
s	entropy change
T_{hm}	at harmonic mean of experimental temperatures
TMS	experimental data measured using the C_1-silica gel column
T_1	at temperature condition 1
T_2	at temperature condition 2
ε	measurement errors
1	condition 1
2	condition 2

References

[1] A.M. Krstulović, P.R. Brown, Reversed-Phase High-Performance Liquid Chromatography, John Wiley & Sons, New York, 1982.
[2] L.C. Sander, S.A. Wise, CRC Crit. Rev. Anal. Chem. 18 (1987) 299.
[3] L.C. Sander, S.A. Wise, J. Chromatogr. A 656 (1993) 335.
[4] C.H. Löchmuller, D.R. Wilder, J. Chromatogr. Sci. 17 (1979) 574.
[5] K.D. Lork, K.K. Unger, Chromatographia 26 (1988) 115.
[6] K.D. Lork, K.K. Unger, H. Brückner, M.T.W. Hearn, J. Chromatogr. 476 (1989) 135.
[7] S.A. Wise, W.E. May, Anal. Chem. 55 (1983) 1479.
[8] K.B. Sentell, J.G. Dorsey, J. Chromatogr. 461 (1989) 193.
[9] H. Colin, J.C. Diez-Masa, G. Guiochon, T. Czajkowska, I. Miedziak, J. Chromatogr. 167 (1978) 41.

[10] W.R. Melander, D.E. Campbell, C. Horváth, J. Chromatogr. 158 (1978) 215.
[11] W.R. Melander, B.K. Chen, C. Horváth, J. Chromatogr. 185 (1979) 99.
[12] G. Vigh, Z. Varga-Puchony, J. Chromatogr. 196 (1980) 1.
[13] M. Kuchar, V. Rejholec, V. Miller, E. Kraus, J. Chromatogr. 280 (1983) 289.
[14] M. Kuchar, E. Kraus, V. Rejholec, V. Miller, J. Chromatogr. 449 (1988) 391.
[15] K.B. Woodburn, L.S. Lee, P.S.C. Rao, J.J. Delfino, Environ. Sci. Technol. 23 (1989) 407.
[16] K. Miyabe, G. Guiochon, J. Phys. Chem. B 103 (1999) 11086.
[17] K. Miyabe, G. Guiochon, Anal. Chem. 71 (1999) 889.
[18] K. Miyabe, G. Guiochon, Adv. Chromatogr. 40 (2000) 1.
[19] K. Miyabe, G. Guiochon, Anal. Chem. 73 (2001) 3096.
[20] K. Miyabe, G. Guiochon, J. Chromatogr. A 919 (2001) 231.
[21] R.R. Krug, W.G. Hunter, R.A. Grieger, J. Phys. Chem. 80 (1976) 2335.
[22] R.R. Krug, W.G. Hunter, R.A. Grieger, J. Phys. Chem. 80 (1976) 2341.
[23] R.R. Krug, Ind. Eng. Chem. Fundam. 19 (1980) 50.
[24] H.M.J. Boots, P.K. de Bokx, J. Phys. Chem. 93 (1989) 8240.
[25] A. Vailaya, C. Horváth, J. Phys. Chem. 100 (1996) 2447.
[26] K. Miyabe, G. Guiochon, J. Chromatogr. A 903 (2000) 1.
[27] A. Tchapla, S. Heron, H. Colin, G. Guiochon, Anal. Chem. 60 (1988) 1443.
[28] A. Tchapla, S. Heron, E. Lesellier, H. Colin, J. Chromatogr. A 656 (1993) 81.
[29] K.K. Unger, Porous Silica, Elsevier, Amsterdam, 1979.
[30] G. Guiochon, S. Golshan-Shirazi, A.M. Katti, Fundamentals of Preparative and Nonlinear Chromatography, Academic Press, Boston, 1994.
[31] D.M. Ruthven, Principles of Adsorption & Adsorption Processes, John Wiley and Sons, New York, 1984.
[32] M. Suzuki, Adsorption Engineering, Kodansha/Elsevier, Tokyo, 1990.
[33] K. Miyabe, G. Guiochon, J. Sep. Sci. 26 (2003) 155.
[34] A. Bondi, J. Phys. Chem. 68 (1964) 441.
[35] C. Horvath, W. Melander, I. Molnár, J. Chromatogr. 125 (1976) 129.
[36] G. Belfort, G.L. Altshuler, K.K. Thallam, C.P. Feerick Jr., K.L. Woodfield, AIChE J. 30 (1984) 197.
[37] B. Lee, Proc. Natl. Acad. Sci. USA 88 (1991) 5154.